

## Chloride Ion Penetrability and Corrosion Behavior of Steel in Concrete with Sustainability Characteristics

R. Corral-Higuera<sup>1,2,\*</sup>, S. P. Arredondo-Rea<sup>1,2</sup>, M.A. Neri-Flores<sup>1</sup>, J. M. Gómez-Soberón<sup>3</sup>,  
J. L. Almaral-Sánchez<sup>2</sup>, J.H. Castorena-González<sup>2</sup>, A. Martínez-Villafañe<sup>1</sup>, F. Almeraya-Calderón<sup>1</sup>

<sup>1</sup> Centro de Investigación en Materiales Avanzados, S.C., Ave. Miguel de Cervantes 120, Complejo Industrial Chihuahua, C.P. 31109, Chihuahua, Chihuahua, México.

<sup>2</sup> Universidad Autónoma de Sinaloa, Facultad de Ingeniería Mochis, Fuente de Poseidón y Ángel Flores s/n, Ciudad Universitaria, C.P. 81223, Sinaloa, México.

<sup>3</sup> Universidad Politécnica de Cataluña, Escuela Politécnica Superior de Edificación de Barcelona, Gregorio Marañón 44-50, C.P. 08020, Barcelona, España.

\*E-mail: [rnm1779@gmail.com](mailto:rnm1779@gmail.com)

Received: 1 February 2011 / Accepted: 18 February 2011 / Published: 1 April 2011

---

As a contributive strategy in the sustainability concrete industry, the durability improving of reinforced concrete structures is currently investigated, as well as the partial or total replacement of its components for recycled materials. For the steel bars, the corrosion is the principal problem of durability in reinforced concrete. Coarse Recycled Concrete Aggregates (RCA), Supplementary Cementing Materials (SCM) byproducts of industrial processes such as fly ash and silica fume were used to produce concrete with sustainability characteristics and for the evaluation of its behavior when it is exposed to chlorides. From the resulting test specimens: electrical resistivity, resistance to charge transfer and resistance to chloride ion penetration, were determined; these parameters specify the minimum necessary properties for concretes, according to regulations, to guarantee their durability when they are exposed to chlorides. The results obtained concluded that the concrete manufactured with 100% RCA and SCM, improves its performance in durability compared with those of conventional concrete.

---

**Keywords:** Recycled aggregate concrete, Supplementary cementing Materials, Electrochemical impedance spectroscopy, Chloride ion penetrability.

### 1. INTRODUCTION

Because of the significant environmental impact that the concrete production causes, and as sustainability contribution for this industry; presently some improvements are being implemented in its durability and its components are being replaced for alternative recyclable materials. Among the most

utilized alternative materials in the concrete production are those that replace the portland cement (Supplementary Cementing Material [SCM]) as silica fume (SF), fly ash (FA) and blast furnace slag. Regarding the aggregates, the Recycled Concrete Aggregates (RCA) are being employed as a natural aggregates replacement. In a concrete, the aggregates constitute, approximately, the 70% of the volume, for that a large quantities of crushed rock, gravel and sand are needed for their extraction, process and transportation, causing important environmental deterioration. The recycling of the concrete obtained from demolition and residues of constructions has been studied since 1950; but from ten years ago to now, the number of investigations about this topic has been increased significantly [1-10]; however the most of them have been focused on the physical-mechanics properties of the RCA and on the concrete made with them (Recycled Aggregate Concrete [RAC]), not studying the effect presented by RCA in the corrosion of the reinforcement steel in RAC exposed to severe environmental conditions, such as the marine environment, for example. At present, the most important pathology in reinforced concrete structures is deterioration by corrosion, caused by the chlorides penetration through concrete, as well as, in a lesser level, by the carbonation of it. The corrosion origins affectations in durability of reinforced concrete structures, it has reported economic losses up to 276 billion dollars by year [11].

On the other hand, concrete with the addition of SCM has reported a good acceptance for its use [12-16], emphasizing the favorable impact of the SCM in the performance of its resistance and durability, as well as in the environmental benefit involved.

The concretes manufactured with recycled materials (SCM or RCA) have different micro-structure and a greater porosity that conventional concretes [17-20]; on the other hand, it has been revealed that the electrical resistivity of concretes is related to the micro-structure of the cementitious matrix (pores distribution) and with the corrosion rate in reinforcement steel [21-23], therefore, the electrical resistivity is employed to evaluate the concrete durability [24]. This research has the objective to analyze the electrochemical and electrical response of the reinforced concrete in order to know the RCA and SCM effect at the beginning of corrosion, and corrosion rate in the reinforcement steel induced by accelerated chlorides ingress. Having the intention to evaluate the corrosion process in reinforced concrete specimens, some tests of Electrochemical Impedance Spectroscopy (EIS) were carried out to determine the electrical resistivity and the resistance to charge transfer. The basics principles of electrochemical corrosion of reinforced concrete is well known [25]. As additional parameter, the resistance to chloride ion penetration by means of rapid chloride penetration test were characterized.

## 2. EXPERIMENTAL METHODOLOGY

Four test specimens series with water-cementing material ratio of 0.48 were manufactured: a) reference specimen manufactured with natural aggregate (NA) and 100% of Portland Cement (PC) Type I [26], b) specimens carried out with coarse RCA and 100% PC, c) specimen carried out with coarse RCA and 30% FA as partial replacement of the PC, and finally, d) specimen manufactured with

coarse RCA and 10% SF as partial replacement of the PC. The characteristics and proportions of each series are shown in Table 1.

**Table 1.** Characteristics and proportion of the test mixtures (by 1m<sup>3</sup> of concrete).

Materials (Kg)	Mixtures identification			
	Natural coarse and fine aggregate	Recycled coarse aggregate, natural sand and SCM		
	NA 100% PC	RA 100% PC	RA 30% FA	RA 10% SF
Water	213.31	213.31	213.31	213.31
Gravel	994.55	870.58	870.58	870.58
Sand	766.17	915.35	915.35	915.35
Cement	444.44	444.44	311.11	400.00
SCM	0.000	0.000	133.33	44.44

2.1. Materials

The RCA has origin in the crushing of concrete test specimens, manufactured with natural aggregates, PC type I, relation water-cement of 0.50 and cured during a 28-day period to temperature and relative humidity (HR) of 23 ± 2 °C and 98 ± 1%, respectively. The natural aggregates proceed from crushed rock (coarse) and river sand (fine), obtained adequate particle size gradation according to the limits established by ASTM C33 [27], some physical properties of these aggregates are shown in Table 2.

**Table 2.** Pphysical properties of the aggregates used in concrete mixtures

Type of aggregate	Relative density (g/cm <sup>3</sup> )	Absorption (%)	Humidity (%)	Fineness module (%)	Maximum size (mm)
Recycled coarse	2.19	6.55	2.14	-	19
Natural coarse	2.50	0.44	0.28	-	19
Natural fine	2.43	4.08	6.66	2.73	4.76

Mexican FA low in calcium, Class F, according to norm ASTM C618 [28], and American SF according to norm ASTM C1240 [29], were employed as SCM. The physical-chemical properties of these materials are shown in Table 3.

**Table 3.** Physico-chemical properties of cementing materials.

Chemical composition (% of weight)								
Material	SiO <sub>2</sub>	Al <sub>2</sub> O <sub>3</sub>	Fe <sub>2</sub> O <sub>3</sub>	CaO	SO <sub>3</sub>	K <sub>2</sub> O	Na <sub>2</sub> O	MgO
CPC	19.94	4.40	2.97	63.50	3.08	0.42	0.12	-
FA	58.84	16.72	3.52	7.35	0.13	0.79	0.94	1.76
SF	95.22	0.08	2.37	0.26	0.11	0.56	0.30	0.24
Physical properties								
	Density (g/cm <sup>3</sup> )	Specific surface, BET (m <sup>2</sup> /kg)		Average size (µm)				
CPC	3.15	1400		15-25				
FA	2.35	1200		5-15				
SF	2.27	19600		0.1-0.2				

2.2. Electrochemical impedance spectroscopy

Having the purpose to evaluate the electrical resistivity and the resistance to charge transfer of the steel-concrete systems studied, three cylindrical test specimens were prepared (h=30 cm, Φ=15 cm) for each mix shown in Table 1. Each test specimen was supplied with two embedded carbon steel bars UNS G10180 with 0.95 cm diameter, with an exposed area of 64 cm<sup>2</sup> and located at 4.5 cm from the outside.

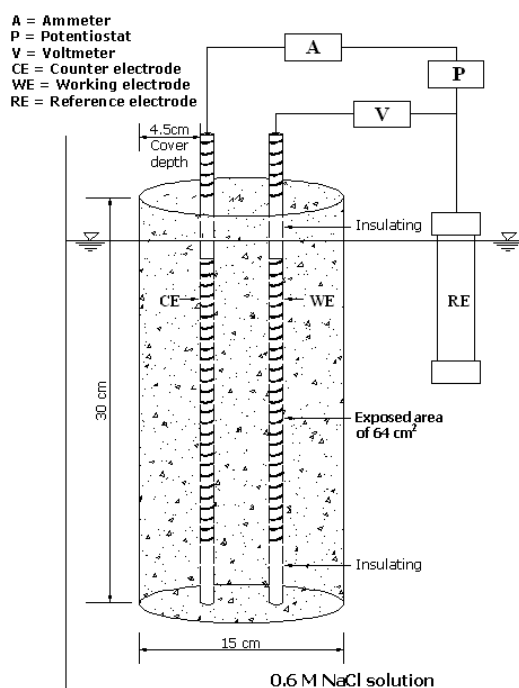


**Figure 1.** Experimental scheme for testing EIS.

The steel bars were stripped and cleaned before their placement. After the 28-day curing time, the specimens were partly immersed (20 cm of depth) in an aqueous solution with 3.5% of NaCl. The immersion period was six months and, from then, the chlorides ingress was accelerated, submitting the specimens to wetted and dried cycles (the test specimen were maintained submerged for three days and, subsequently, they were submitted to drying in a chamber with ventilation to 40° C). The electrolytic Resistance (Re) variation, correlative with the concrete electrical resistivity ( $\rho$ ), and the Resistance to charge transfer (Rct) variation, correlative with the corrosion current density ( $i_{corr}$ ) of the reinforcement, were evaluated each month in submerged conditions.

The evaluation of the parameters (Re and Rct) was carried out for EIS in a potentiostat/galvanostat/zra of ACM Instruments; the test parameters were a potential of 10 mV of amplitude to maintain the system linearity in a range of frequencies from 1 mHz to 10 kHz. The experimental set up is shown in Figure 1.

The results of EIS were represented with Nyquist diagrams [Figure 2 a)], and an equivalent electric circuit (EEC), Randles type, as the one shown in Figure 2 b) was used to determine with precision the intersection value at low frequencies of the curve with the real impedance axis, and thus to be able to calculate Rct.

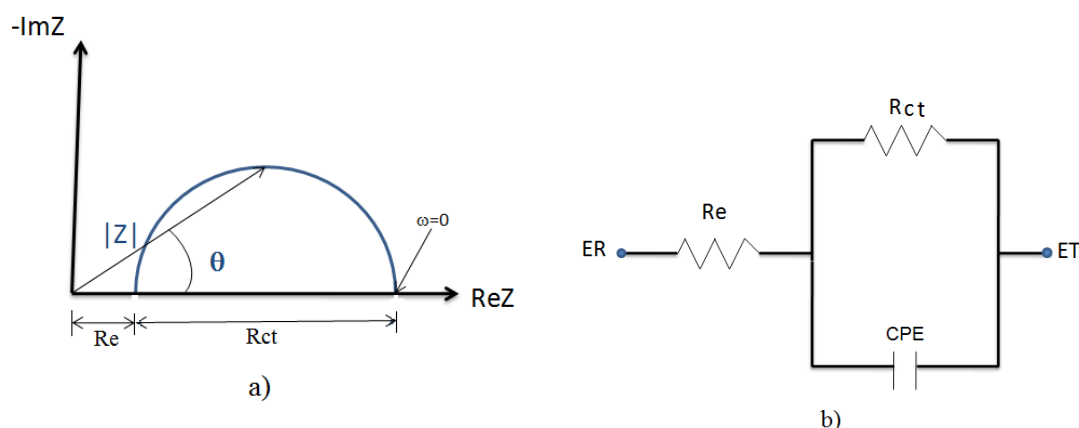


**Figure 2.** a) Ideal Nyquist diagram, b) EEC used to simulate experimental results of EIS.

The resultant Rct and the obtained Re from the intersection at high frequencies of the Nyquist diagrams with the real impedance axis, were used to determine  $i_{corr}$  and  $\rho$ , respectively. Utilizing Equation 1 [30]  $i_{corr}$  was calculated, where B is the Tafel constant, with recommended value [31-34] of 0.052 V for the reinforcement steel passive corrosion and 0.026 V for active corrosion;  $\rho$  was obtained from Equation 2, where  $C_c$  is a cell constant that depends of the conductor geometry and its value is 58.47 cm [35].

$$i_{corr} = \frac{B}{Rct} \tag{1}$$

$$Re = \rho \cdot C_c \tag{2}$$

2.3. Resistance to chloride ion penetration

The Rapid Chloride Penetration Test (RCPT) was performed in agreement with ASTM C 1202 [36]. The tests were carried out in 90-day-curing test specimen (h=5 cm, Φ=10 cm) extracted from the central part of concrete cylinders (h=20 cm). The test specimen curved surface was covered with waterproofing, and after one drying hour, they were introduced in a dryer chamber both faces exposed to a vacuum pressure of 1mm Hg (133 Pa) for three hours; subsequently, the chamber was filled with deoxygenated water maintaining the vacuum pressure for an hour, finally, their immersion was maintained for 20 hours more without chamber pressure. After a 24-hour period of their preparation, the test specimens were placed between two acrylic cells connected to a potentiostat. One of the cells was filled with aqueous solution with 0.3 N of NaOH and the other with aqueous solution with 3% of NaCl. The cells were connected to the voltage supply source, where the electrode of the cell with NaCl functioned as cathode and the NaOH electrode functioned like anode. A constant voltage of 60 V was applied for six hours and a record of the flow was registered each half an hour. The test configuration is shown in Figure 3.

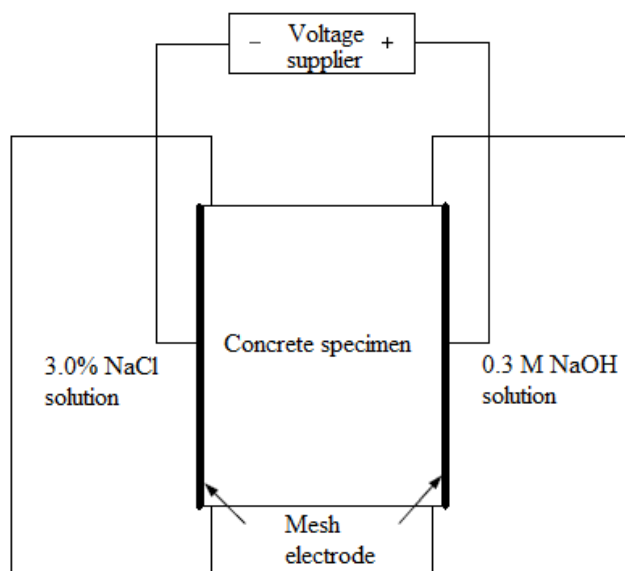


Figure 3. Experimental set up for RCPT

The total passed charge (Q) through the test specimen was calculated with Equation 4 according to the trapezoidal rule.

$$Q = 900x(I_0 + 2I_{30} + 2I_{60} + \dots + 2I_{330} + 2I_{360}) \tag{4}$$

Where: Q is expressed in Coulombs, and  $I_n$  is the flow (A) to n minutes after the potential is applied. Since Q is related to the concrete resistance to chloride ion penetration, this was determined by means of the qualitative criterion proposed in ASTM C1202 (Table 4).

**Table 4.** Chloride ion penetrability based on charge passed

Charge passed (C)	Chloride ion penetrability
> 4000	High
2000 – 4000	Moderate
1000 – 2000	Low
100 – 1000	Very low
< 100	Negligible

### 3. RESULTS AND DISCUSSION

#### 3.1. Electrochemical impedance spectroscopy.

The dielectric and electrochemical properties of the concrete-steel systems to 3, 6, 9 and 12 months of exposition are represented in Nyquist diagrams in Figure 4.

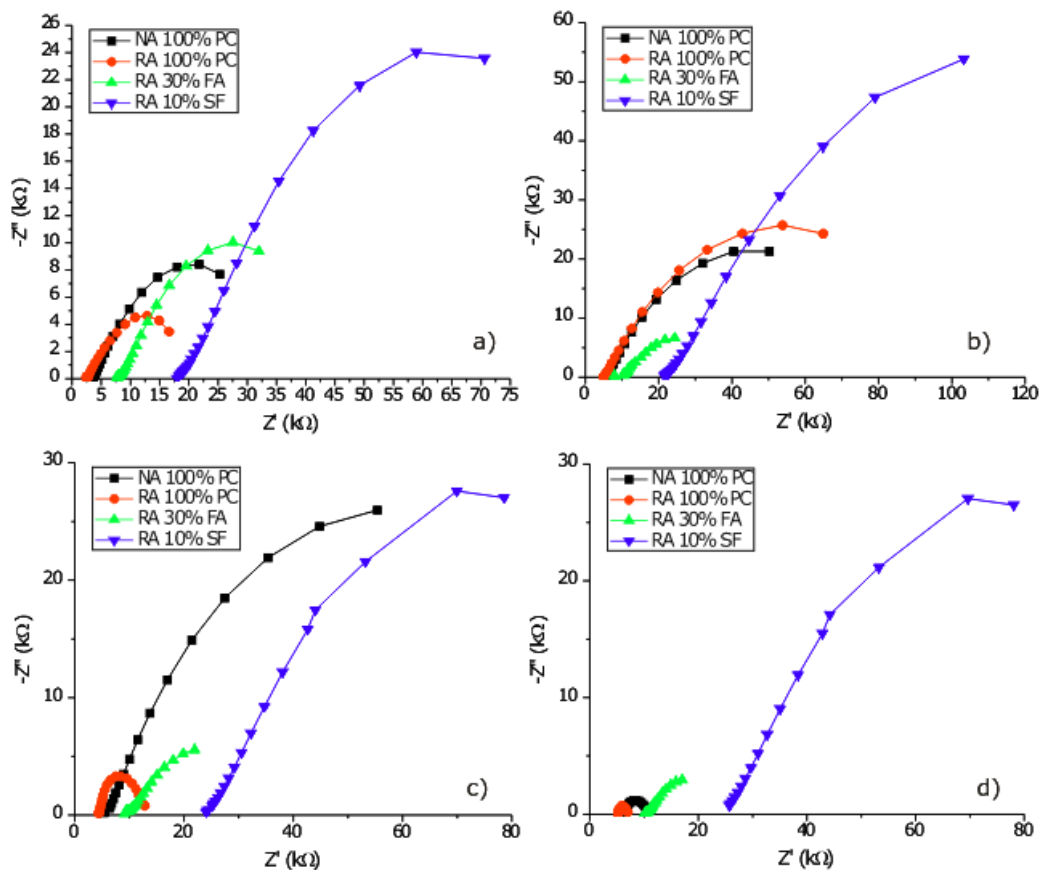


**Figure 4.** Nyquist diagram for concrete-steel systems to different age of exposure: a) 3 months, b) 6 months, c) 9 months y d) 12 months

It is observed the RCA influence in the Re (intersection in the curve at high frequencies) and in the Rct (diameter of the semicircle or arch). The RA 100% PC system presents the lower values of Re (from 1.22 to 3.30 x10<sup>2</sup> kΩ-cm<sup>2</sup>) indicating that the use of 100% of RCA enlarges the electric conductivity in concretes. Nevertheless, when cement is replaced by FA and SF, the concrete Re increases in a significant form (diminishes the electrical conductivity), especially using SF (of 4.6 x10<sup>2</sup> a 1.48 x10<sup>3</sup> kΩ-cm<sup>2</sup>). With regard to the Rct, a similar behavior is appreciated, being the RCA 10% SF system the one that reports the maximum values of Rct during the exposition time (from 6.25 x10<sup>2</sup> a 6.79 x10<sup>3</sup> kΩ-cm<sup>2</sup>, meanwhile the RA 100% PC system reported the minimum Rct values (8.64 x 10<sup>2</sup> a 7.98 x 10<sup>1</sup> kΩ-cm<sup>2</sup>).

In Figure 5, the ρ as a function of the exposure time is shown, it is possible to confirm that the use of 100% of RCA originates increments in the electric conductivity of concrete, this is attributed to the porosity increment reported in the concrete with RCA [17-20] by the presence of new interfacial transition zones that facilitate the ionic conduction. The ρ in systems without SCM (NA 100% PC and RA 100% PC) do not surpass the upper limit [37] of the 10 kΩ-cm. For systems with SCM, is important the positive effect of them in the ρ of the concrete; the ρ of the RA 30% FA system is the double that the one in systems without SCM, meanwhile the one of RA 10% SF system is four times larger. Similar results were found by G. Fajardo et al. [38].

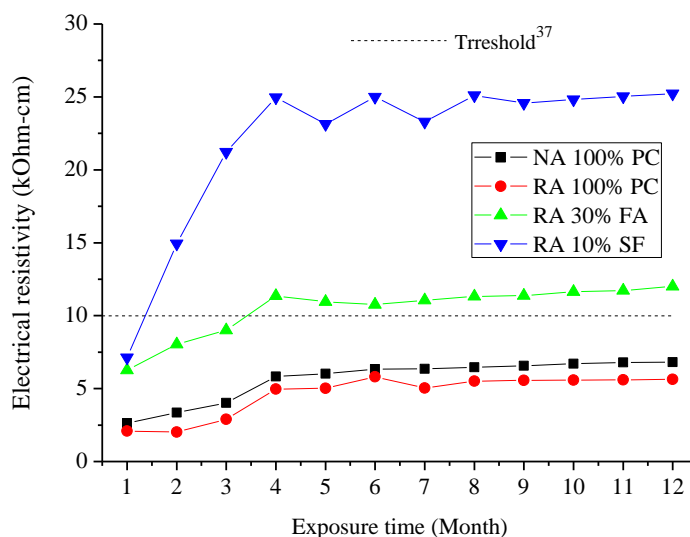


**Figure 5.** Evolution of electrical resistivity as a function of exposure time

Figure 5 shows that during the first three months of experiment, the ρ of systems with SCM is increased quickly, and then, it stabilizes; this behavior can be explained assuming that the reactions approach the equilibrium when a period of about 90 days of exposition has passed. The increase of ρ in systems with SCM is attributed to the decrease of the porous system produced by the increase in the SCH formation and the reduction in CH formation product of the pozzolanic reaction between this last and the SiO<sub>2</sub> contained in the SCM. It can be observed in Table 3 that SF is about of 100 times thinner

than cement and FA, and contributes in greater quantity of SiO<sub>2</sub>. The use of pozzolanic materials reduce the porosity in the cementitious matrix [12,16,39,40] which is directly related to the electrical resistivity.

The  $i_{corr}$ , results determined from the values of Rct are presented in Figure 6, they verified the corrosion resistance in the steel-concrete systems of this study. It is observed that in the fourth month of trial, an inflection point between two corrosion states with different degree of activity is located; this consideration is attributed to, from this point, the reactions of pozzolanic hydration of the cement and that SCM reached an equilibrium state, and because of it, the velocity is stabilized. It is also observed that RA 10% SF system has the greater corrosion resistance, in spite of the fact that its corrosive activity was the biggest in the first month, diminishing significantly during the subsequent months until having the minimum corrosion level (0,004  $\mu\text{A}/\text{cm}^2$ ) in the sixth month of trial, with a period-of-test average of 0,016  $\mu\text{A}/\text{cm}^2$ ; besides it is also observed that the use of SF delays, in an significant form, the beginning of corrosion, because it remains in a passive state until the twelfth month. On the other hand, the RA 100% PC system reports the maximum levels of corrosion (from 0,044 to 0,060  $\mu\text{A}/\text{cm}^2$ ) in the third month; and although among the fourth to eighth month its corrosive activity diminishes considerably, it registers the  $i_{corr}$  major average (0,102  $\mu\text{A}/\text{cm}^2$ ) for the complete period; this classifies it as the system with smaller corrosion resistance and it clarifies the RCA negative effect in the susceptibility to reinforcement corrosion since its corrosive activity passed from the passive state to the active state in the eighth month (before that any another system). The RA 30% FA system reports low corrosion levels during the two first months of test (from 0,022 to 0,037  $\mu\text{A}/\text{cm}^2$ ), maintaining its activity in that level for the subsequent months; its average  $i_{corr}$  was of 0,026  $\mu\text{A}/\text{cm}^2$ , and it can be observed that the use of FA delays the beginning time of reinforcement corrosion.

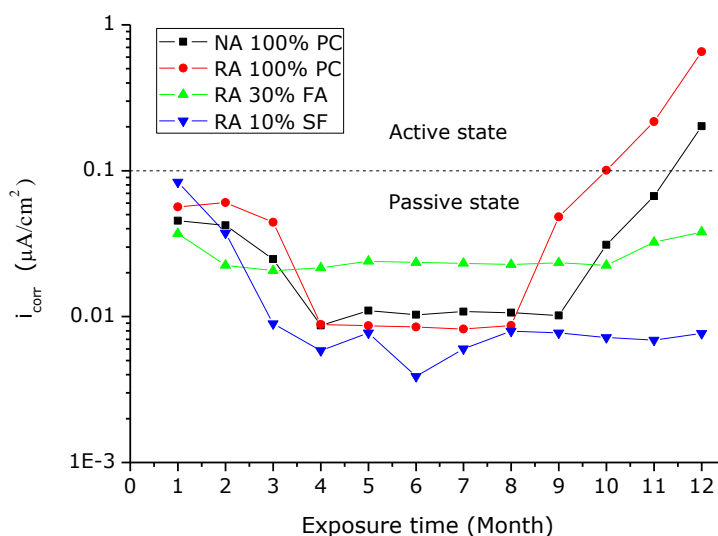


**Figure 6.** Variation of corrosion current density as a function of exposure time

The previous results indicate that although a significant difference of  $\rho$  in systems with SCM exists, its corrosion resistance is maintained in the same magnitude level; this is attributable to the high

content of  $\text{Al}_2\text{O}_3$  ( $\cong 17\%$ ) of the FA, contributing to form Friedel salt or tricalcium chloroaluminate ( $3\text{CaO}\cdot\text{Al}_2\text{O}_3\cdot\text{CaCl}_2\cdot 10\text{H}_2\text{O}$ ). Therefore, the FA addition generates, in the cementitious matrix, a higher content of Friedel salt and, consequently, lower levels of free chlorides, which in this case are responsible of the corrosion located in the reinforcement steel. The above was verified by means of XRD and as it is observed in Figure 7, this compound was detected (higher peak in  $2\theta = 11.18$ ) in each one of the mix (with 100% PC and replacing PC with 30% FA); nevertheless, higher intensities are observed for the mix with FA than for the mix with 100% PC.

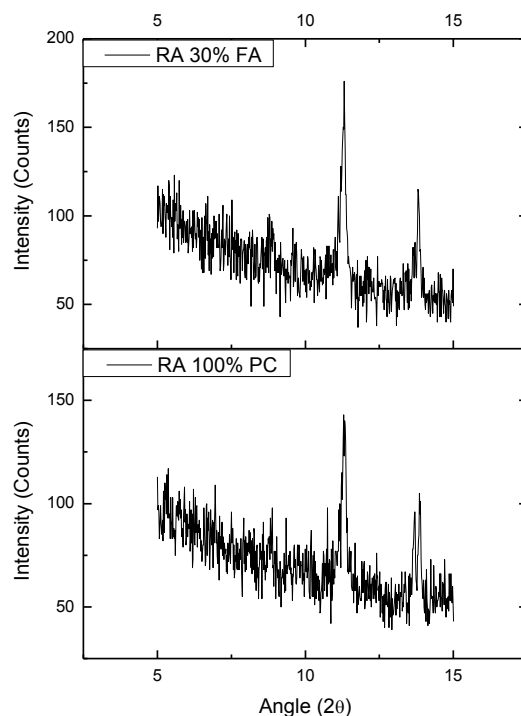


**Figure 7.** X Rays patterns – Friedel salt

### 3.2. Resistance to chloride ion penetration

In Figure 8, the results of passed charge according to the ASTM C1202 procedure of test are presented. The results indicate, first, the use of 100% of RCA decreases its capacity to resist the penetration of the chloride ion in approximately 30% in respect of the conventional concrete. On the other hand, it can be observed that the use of FA and SF provides to the concrete a great capacity to inhibit the chloride ions penetration, because the passed charge in the mix RA 30% FA and RA 10% SF is three and five times smaller, respectively, than the mix RA 100% PC. According to the criterion proposed by ASTM C1202 (Table 4), the mix without SCM presents a high penetrability of the chloride ion because it surpasses the 4000 Coulombs, meanwhile the penetrability in mix with SCM is classified as low because it has between 1000 and 2000 Coulombs. These results are compatible with the ones reported by K.Y. Ann et al. [12].

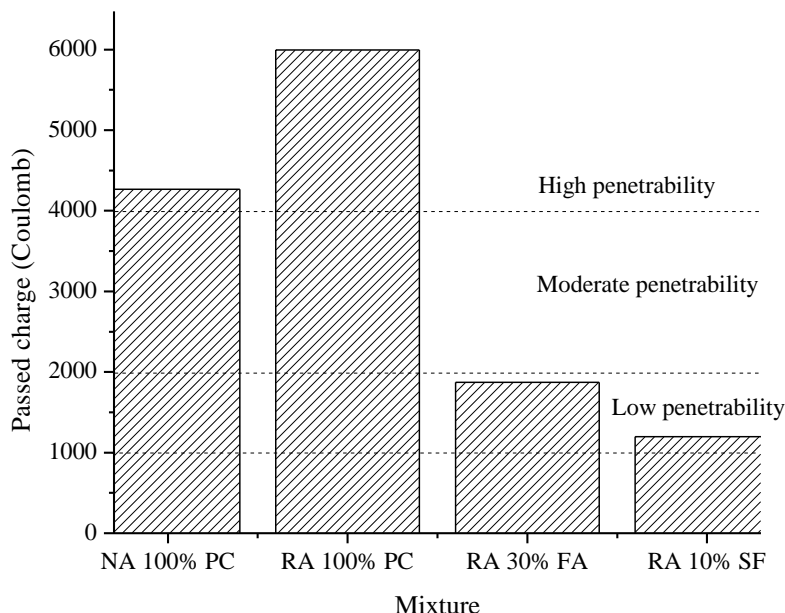


**Figure 8.** Resistance to chloride ion penetration

The high resistance to chloride ion penetration in the mix with SF is due to the greater densification of the cementitious matrix observed in Figure 9c (micrography obtained by SEM), which reduces significantly the capillary porosity, restricting the chlorides permeability. For the mix with FA, in spite of the fact that its cementitious matrix has similar compactness than the mix with 100% PC (Figures 9a and 9b), the formation of Friedel salt in greater quantity and the obstruction of pores with particles of FA without reacting (spheres in Figure 9b), contribute to a smaller permeability of chloride ions.

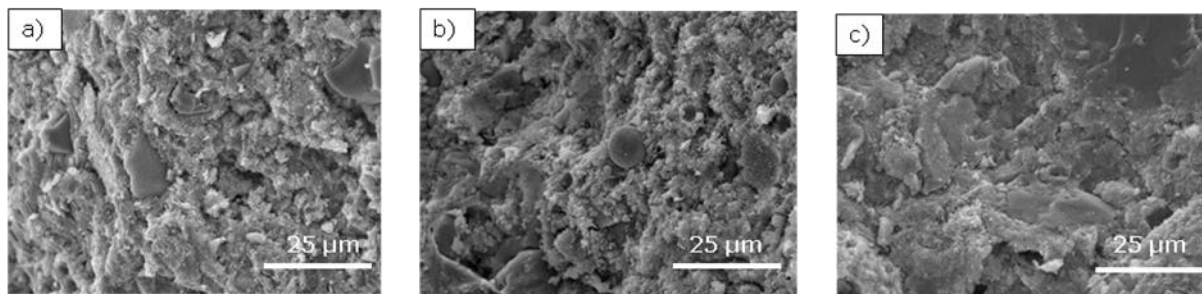


**Figure 9.** Microstructure of cementing matrix to 90 days of hydration: a) 100% PC, b) 70% PC – 30% FA, c) 90% PC – 10% SF.

#### 4. CONCLUSIONS

- The use of 100% of RCA decreases the corrosion resistance of reinforcement in concrete; nevertheless, the use of SCM in concretes with 100% of RCA increases the corrosion resistance by the ingress of water-soluble chlorides.

- The 100% replacement of natural aggregate for RCA decreases the electric resistivity of concretes and the beginning time of the reinforcement corrosion, besides increasing the corrosion rate of it.
- The fly ash and the silica fume duplicate and quadruple, respectively, the electric resistivity of concretes; they delay the beginning of reinforcement corrosion and decrease its velocity.
- Although the magnitude of the electric resistivity in concretes with silica fume is the double that the one in concretes with fly ash, both have similar corrosion resistance, due to high  $Al_2O_3$  of fly ash contained, it contributes to form Friedel salt and reduces the permeability of the chloride ion.
- The RCPT results indicate that concretes manufactured with RCA have a more open structure of pores than conventional concretes. The use of 30% FA and 10% HS outcomes in a decrement in the total passed charge through the concrete in three and five times, respectively, it signifies a considerable increment in the resistance to chloride ion penetration.

#### AKNOWLEDGEMENTS

The authors thank to CONACYT by its support to accomplish their PhD studies, with the scholarship number 185273. Also to the Universidad Autónoma de Sinaloa and DGIP by the scholarship offered in its young PhD-professionals program and to the Advanced Materials Research Center, SC by the support in the samples characterization and analysis of results.

#### References

1. A.Ajdukiewicz, A. Kliszczewicz, *Cement and Concrete Composites*, 24 (2002) 269.
2. H. Chen, T. Yen, K. Chen, *Cement and Concrete Research*, 33 (2003) 125.
3. A.Katz, *Cement and Concrete Research*, 33 (2003) 703.
4. C.S. Poon, Z.H. Shui, L. Lam, H. Fok, S.C. Kou, *Cement and Concrete Research*, 34 (2004) 31.
5. I.Topçu, S. Sengel, *Cement and Concrete Research*, 34 (2004) 1307.
6. T. Tu, Y. Chen, C. Hwang, *Cement and Concrete Research*, 36 (2006) 943.
7. I.Martínez, C. Mendoza, *Ingeniería Investigación y Tecnología*, 7 (2006) 151.
8. K. Rahal, *Building and Environment*, 42 (407) (2007) 407.
9. M. Casuccio, M.C. Torrijos, G. Giaccio, R. Zerbino, *Construction and Buildings Materials*, 22 (7) (2008) 500.
10. A.K. Padmini, K. Ramamurthy, M.S. Mathews, *Construction and Buildings Materials*, 23 (2009): 829.
11. Administration Federal Highway, *Corrosion Costs and Preventative Strategies in the United States*. 2002, Publication No. FHWA-RD-01-156
12. K.Y. Ann, H.Y. Moon, Y.B. Kim, J. Ryou, *Waste Management*, 28 (2008) 993.
13. B. González, F. Martínez, *Building and Environment*, 43 (2008) 429.
14. S.C. Kou, C.S. Poon, D. Chan, *Materials and Structures*, 41 (2008) 1191.
15. M.L. Berndt, *Construction and Buildings Materials*, 23 (2009) 2606.
16. V.Corinaldesi, G. Moriconi, *Construction and Buildings Materials*, 23 (2009) 2869.
17. J.M.V. Gómez, *Cement and Concrete Research*, 32 (2002) 1301.
18. C.S. Poon, Z.H. Shui, L. Lam, *Construction and Buildings Materials*, 18 (2004) 461.
19. V.W.Y. Tam, X.F. Gao, C.M. Tam, *Cement and Concrete Research*, 35 (2005) 1195.
20. M. Etxeberria, E. Vazquez, A. Mari, *Magazine of Concrete Research*, 58 (2006) 683.

21. P.J. Tumidajski, A.S. Shumacher, S. Perron, P. Gu, J.J. Beaudoin, *Cement and Concrete Research*, 26 (1996) 539.
22. P.J. Tumidajski, *Cement and Concrete Research*, 35 (2005) 1262.
23. R. Polder, C. Andrade, B. Elsener, O.E. Vennesland, J. Gulikers, R. Weidert, M. Raupach, *Materials and Structures*, 33 (2000) 603.
24. Song H.W. and Saraswathy, *International Journal of Electrochemical Science*, 2 (2007) 1.
25. Dao L.T.N., Dao V.T.N., Kim S.H. and Ann K.Y., *International Journal of Electrochemical Science*, 5 (2010) 302.
26. ASTM International. ASTM C150-09, *Standard Specification for Portland Cement*. ASTM International, (2009).
27. ASTM International, ASTM C33-08, *Standard Specification for Concrete Aggregates*. ASTM International, 2008.
28. ASTM International. ASTM C618-08, *Standard Specification for Coal Fly Ash for Use as a Mineral Admixture in Concrete*. ASTM International, (2008).
29. ASTM International, ASTM C1240-05, *Standard Specification for Silica Fume Used in Cementitious Mixtures*. ASTM International, (2005).
30. M. Stern, A. Geary, *Journal of the electrochemical society*, 104 (1957) 56.
31. R.K. Dhir, M.R. Jones, M.J. McCarthy, *Cement and Concrete Research*, 23 (1993) 1443.
32. J.A. González, E. Ramírez, A. Bautista, S. Feliú, *Cement and Concrete Research*, 26 (1996) 501.
33. K.R. Gowers, S.G. Millard, *Corrosion Science*, 35 (1993) 1593.
34. P.S. Mangat, B.T. Molloy, *Materials and Structures*, 25 (1992) 404.
35. S.P. Arredondo-Rea, R. Corral-Higuera, M.A. Neri-Flores, J.M. Gómez-Soberón, F. Almeraya-Calderón, J.H. Castorena-González and J.L. Almaral-Sánchez, *International Journal of Electrochemical Science*, 6 (2011) 475.
36. ASTM International, ASTM C1202-10, *Standard Test Method for Electrical Indication of Concrete's Ability to Resist Chloride Ion Penetration*: ASTM International; 2010.
37. C. Andrade, C. Alonso, *Construction and Building Materials*, 10 (1996) 315.
38. G. Fajardo, P. Valdez, J. Pacheco, *Construction and Building Materials*, 23 (2009) 768.
39. M. Montemor, A.M.P., Simões, M.M. Salta, *Cement and Concrete Composites*, 22 (2000) 175.
40. W. Sun, Y. Zhang, S. Lui, Y. Zhang, *Cement and Concrete Research*, 34 (2004) 1781.